1-1-2001

Ancient drainage basin of the Tharsis region, Mars: Potential source for outflow channel systems and putative oceans or paleolakes

J. M. Dohm

J. C. Ferris

V. R. Baker

R. C. Anderson

T. M. Hare

See next page for additional authors

JOURNAL OF GEOPHYSICAL RESEARCH, VOL. 106, NO. E12, PAGES 32,943–32,958, DECEMBER 25, 2001

Ancient drainage basin of the Tharsis region, Mars: Potential source for outflow channel systems and putative oceans or paleolakes

J. M. Dohm,[1] J. C. Ferris,[1] V. R. Baker,[1,2] R. C. Anderson,[3,4]
T. M. Hare,[5] R. G. Strom,[2] N. G. Barlow,[6] K. L. Tanaka,[5]
J. E. Klemaszewski,[7] and D. H. Scott[8]

Abstract. Paleotopographic reconstructions based on a synthesis of published geologic information and high-resolution topography, including topographic profiles, reveal the potential existence of an enormous drainage basin/aquifer system in the eastern part of the Tharsis region during the Noachian Period. Large topographic highs formed the margin of the gigantic drainage basin. Subsequently, lavas, sediments, and volatiles partly infilled the basin, resulting in an enormous and productive regional aquifer. The stacked sequences of water-bearing strata were then deformed locally and, in places, exposed by magmatic-driven uplifts, tectonic deformation, and erosion. This basin model provides a potential source of water necessary to carve the large outflow channel systems of the Tharsis and surrounding regions and to contribute to the formation of putative northern-plains ocean(s) and/or paleolakes.

1. Introduction

Stratigraphic, tectonic, and erosional records, compiled through geological mapping investigations at regional and local scales, demonstrate a significant contribution of magmatic-driven processes to the dynamic geologic history of Mars [for example, *Mouginis-Mark*, 1985; *Scott and Tanaka*, 1986; *Greeley and Guest*, 1987; *Baker et al.*, 1991; *Crown et al.*, 1992; *Scott et al.*, 1993; *Robinson et al.*, 1993; *Crown and Greeley*, 1993; *Gregg et al.*, 1998]. These processes are perhaps best exemplified at Tharsis and the surrounding regions in the western hemisphere [*Frey*, 1979; *Wise et al.*, 1979; *Plescia and Saunders*, 1982; *Solomon and Head*, 1982; *Scott and Tanaka*, 1986; *Morris and Tanaka*, 1994; *Scott and Zimbelman*, 1995; *Anderson et al.*, 1998, 2001; *Scott et al.*, 1998; *Golombek*, 2000; *Solomon and Head*, 2000], where pulses of magmatic activity associated with the development of the Tharsis Magmatic Complex (TMC) [e.g., *Dohm et al.*, 2000a, 2000b] may have triggered catastrophic floods and short-lived climatological perturbations [*Baker et al.*, 1991, 2000; *Baker*, 2001].

The Tharsis magmatic complex is composed of numerous components that formed during specific stages of the complex's development (Plates 1 and 2), including volcanic constructs of varying sizes and extensive lava flow fields, large igneous plateaus, fault and rift systems of varying extent and relative age of formation, gigantic outflow channel systems, vast canyon systems, and local and regional centers of tectonic activity. Many of the local and regional centers of tectonic activity [*Anderson et al.*, 1998, 2001; *Anderson and Dohm*, 2000] are interpreted to be the result of magmatic-related activity, including uplift, faulting, dike emplacement, volcanism, and local hydrothermal activity [*Dohm et al.*, 1998, 2000b, 2000d, 2001a; *Dohm and Tanaka*, 1999]. The geologic history of the numerous components of the Tharsis magmatic complex, which has been analyzed in detail by numerous investigators (see Plate 1), is incorporated into the analyses and interpretations that follow.

Inasmuch as the relative age of formation of the primary components of the complex are generally understood, the general stratigraphy established, and the high-resolution topography of present-day Mars known, the features and materials can be "backstripped" systematically from their present configuration. This provides an approximate sequential three-dimensional (3-D) view of the paleotopography at the cessation of each of the five stages of the complex's development (Plates 3–7). Stage information correlates with the scheme devised by *Dohm and Tanaka* [1999] (see Plates 1 and 2).

The purpose of the 3-D visualization and quasi-quantitative backstripping is not to generate a quantitatively accurate reconstruction of Martian paleotopography at discrete time steps. Such a reconstruction may well be possible at a future date when more data become available. However, the more qualitative visualizations employed in this study serve to summarize inferences made from geological mapping and analyses and synthesis of published map information. This summary, really an illustrated working hypothesis, leads to the identification of an ancient, gigantic drainage basin that persists through much of the history of the region. Moreover, the drainage basin, once identified, is found to be consistent with a diverse series of other observations. The overall coherence of

[1]Department of Hydrology and Water Resources, University of Arizona, Tucson, Arizona, USA.
[2]Lunar and Planetary Laboratory, Department of Planetary Science, University of Arizona, Tucson, Arizona, USA.
[3]Jet Propulsion Laboratory, Pasadena, California, USA.
[4]Lunar and Planetary Laboratory, University of Arizona, Tucson, Arizona, USA.
[5]U.S. Geological Survey, Flagstaff, Arizona, USA.
[6]Robinson Observatory, Department of Physics, University of Central Florida, Orlando, Florida, USA.
[7]Department of Geology, Arizona State University, Tempe, Arizona, USA.
[8]Deceased August 9, 2000.

Paper number 2000JE001468.
0148-0227/01/2000JE001468$09.00

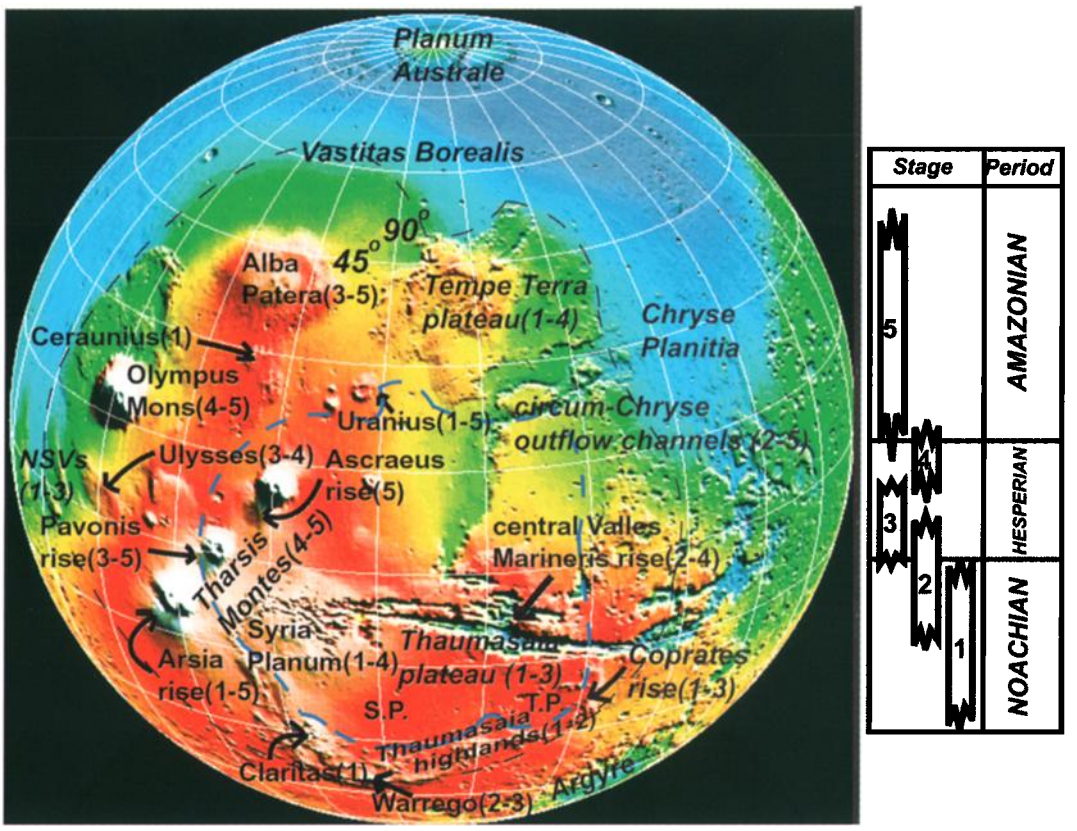

Plate 1. Mars Orbiter Laser Altimeter (MOLA) shaded relief map of the western hemisphere of Mars (courtesy of the MOLA Science Team). Shown are the major geologic features of the Tharsis Magmatic Complex (TMC) and their stages of development (stage assignments 1–5 of *Dohm and Tanaka* [1999] and *Dohm et al.* [2001a] correlated with the time-stratigraphic age assignment: Noachian, Hesperian, and Amazonian periods of *Tanaka* [1986]), based on numerous detailed geologic investigations [e.g., *Milton*, 1974; *Baker and Milton*, 1974; *Plescia et al.*, 1980; *Plescia and Saunders*, 1982; *Scott and Tanaka*, 1986; *Tanaka*, 1986; *Tanaka and Davis*, 1988; *Frey and Grant*, 1990; *Tanaka*, 1990; *Scott and Dohm*, 1990a, 1990b; *Baker et al.*, 1991; *Witbeck et al.*, 1991; *Chapman et al.*, 1991; *Morris et al.*, 1991; *Lucchitta et al.*, 1992; *DeHon*, 1992; *Scott*, 1993; *Gulick*, 1993; *Morris and Tanaka*, 1994; *Schultz and Tanaka*, 1994; *Rotto and Tanaka*, 1995; *Scott and Zimbelman*, 1995; *Scott et al.*, 1995; *Rice and DeHon*, 1996; *Chapman and Tanaka*, 1996; *Scott and Dohm*, 1997; *Scott et al.*, 1998; *Dohm et al.*, 1998; *Anderson et al.*, 1998; *Dohm and Tanaka*, 1999; *Nelson and Greeley*, 1999; *McKenzie and Nimmo*, 1999; *Anderson and Dohm*, 2000; *Dohm et al.*, 2000b; *Chapman and Lucchitta*, 2000; *Head et al.*, 2000; *Baker et al.*, 2001; *Dohm et al.*, 2001a, 2001b; *Anderson et al.*, 2001]. Also shown are Solis and Thaumasia Planae (S.P. and T.P., respectively), approximated margins of the TMC (black dashed outline), northwestern slope valleys (NSVs), and the Noachian drainage basin (blue dashed outline).

these observations can be considered to be a tentative confirmation of utility for the basin hypothesis. While the quantitative confirmation of detailed validity for various reconstructions is beyond the scope of this preliminary study, such reconstructions would be among the several possible follow-ons to the present study.

2. Three-Dimensional Portrayal of the Evolution of the Tharsis Magmatic Complex

A 3-D visualization program (Bryce 4 by the MetaCreations Corporation) provides a heuristic representation of the geological evolution of the Tharsis Magmatic Complex. Although this program cannot modify present-day Mars Orbiter Laser Altimeter (MOLA)-based topography in absolute elevation values, it can mold surfaces and render and animate 3-D scenes. Visual appearances for each of the five major stages of activity of the Tharsis Magmatic Complex were generated using the above referenced topographic, stratigraphic, paleoerosional, and paleotectonic information. This information includes spatial and temporal relations among shield volcanoes, igneous plateaus, magmatic-driven centers of tectonic activity, fault and rift systems, and lava flow fields. In this process, features and materials of a known relative age were systematically backstripped from their present MOLA-based configuration, providing approximate sequential views of the paleotopography at the cessation of each of the five stages of the complex's development.

We emphasize that these illustrations are qualitative at this point. They represent a working hypothesis, based on our interpretation of the geologic mapping and analyses and synthesis of published map information, that should be tested with quantitative data as these become more available in formats that can be related to the geology. We also emphasize that the thicknesses and areal extent of features/materials are approximated, because geologic histories for Mars are established

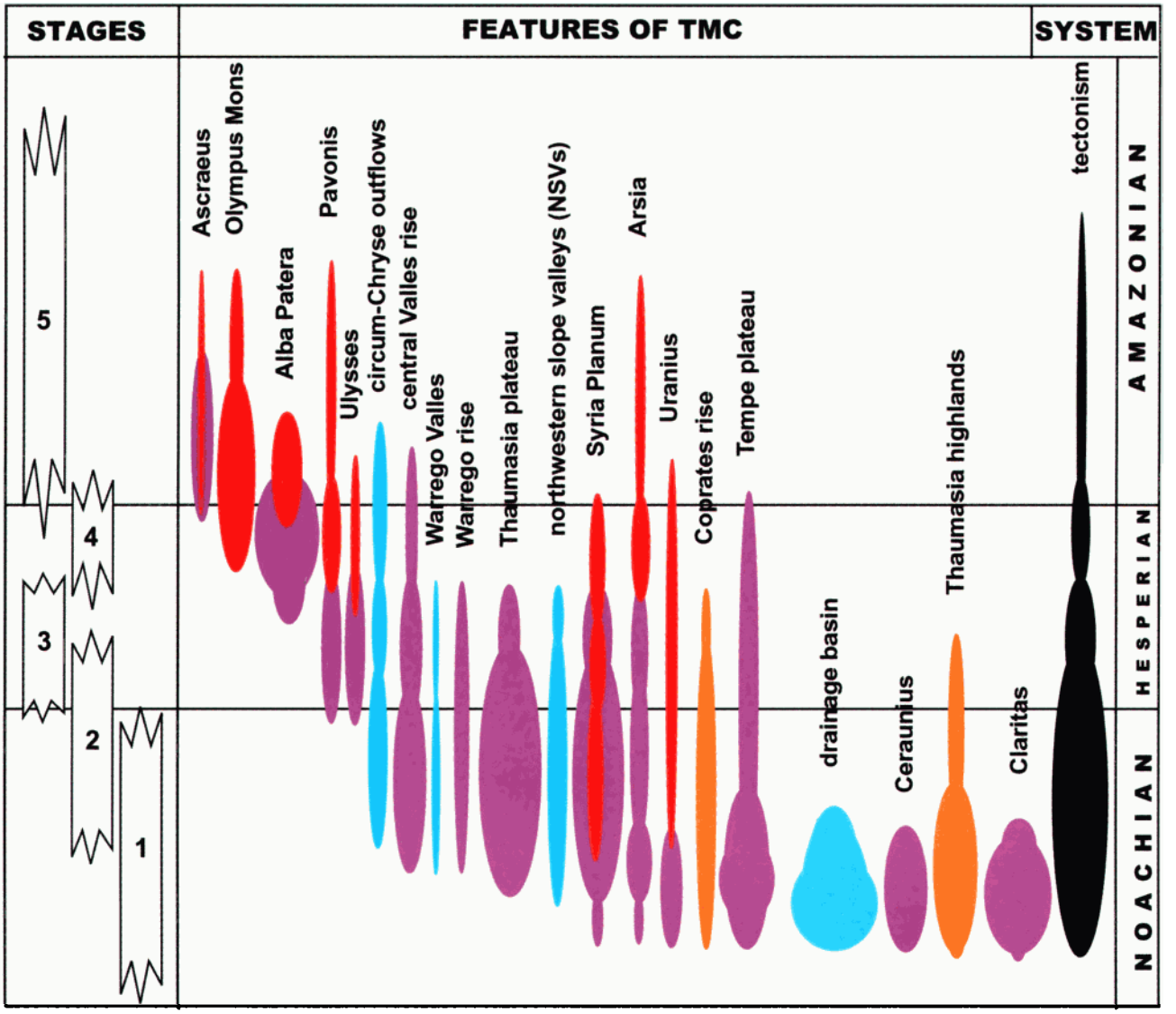

Plate 2. Chart comparing the stages of geologic activity in the Tharsis Magmatic Complex region with major geologic features, including the Noachian drainage basin (correlates to Plate 1). Size of the solid areas is roughly proportional to the degree of exposed deformation. Violet, centers of tectonic activity interpreted to be the result of magmatic-driven uplift and local volcanism, dike emplacement, and hydrothermal activity; orange, mountain building; blue, water; red, primarily emplacement of shield-forming and lava-field-forming lavas. Note that the commencement and/or end of activity of the components of the complex are not absolutely constrained and that features such as the shield volcanoes of Tharsis Montes and Olympus Mons could be presently active.

through photogeologic mapping and relative-age determination of surfaces and structures. Even on Earth, paleotopographic reconstructions are difficult where a much richer set of tools for analyzing the geologic record can be used, including field mapping and absolute dating of rocks.

In addition to utilizing published geologic information and cross sections (e.g., Plates 8a–8c), our reconstructions make use of MOLA-derived topographic profiles (e.g., Plates 9–11) to best estimate thicknesses and areal extents of features and materials. Plates 9 and 10, for example, show substantial rises in the central and western parts of Valles Marineris, which are located near the central part of the proposed drainage basin. These rises, which have been identified as centers of tectonic activity [*Anderson et al.*, 1998, 2001; *Anderson and Dohm*, 2000], are interpreted to be the result of magmatic-driven uplifts and local volcanism and hydrothermal activity along large structural discontinuities in the Martian crust [*Dohm et al.*, 1998; *Anderson and Grimm*, 1998; *Dohm et al.*, 2001a]; the Late Noachian-Hesperian centers of tectonic activity postdate the proposed drainage basin.

We started from Stage 5 (present day, Amazonian Period; Plate 3) by importing the MOLA Experiment Gridded Data Record (EGDR) and ended with Stage 1 (Noachian Period; Plate 7). For example, for the Late Hesperian/Amazonian (Stages 4–5; Plates 4 and 3, respectively), gigantic volcanic constructs of Tharsis Montes and Olympus Mons and their associated lavas flow fields were removed from the Noachian/Early Hesperian (Stages 1–3) reconstructions using Bryce surface editing tools (Plates 5–7, respectively). In

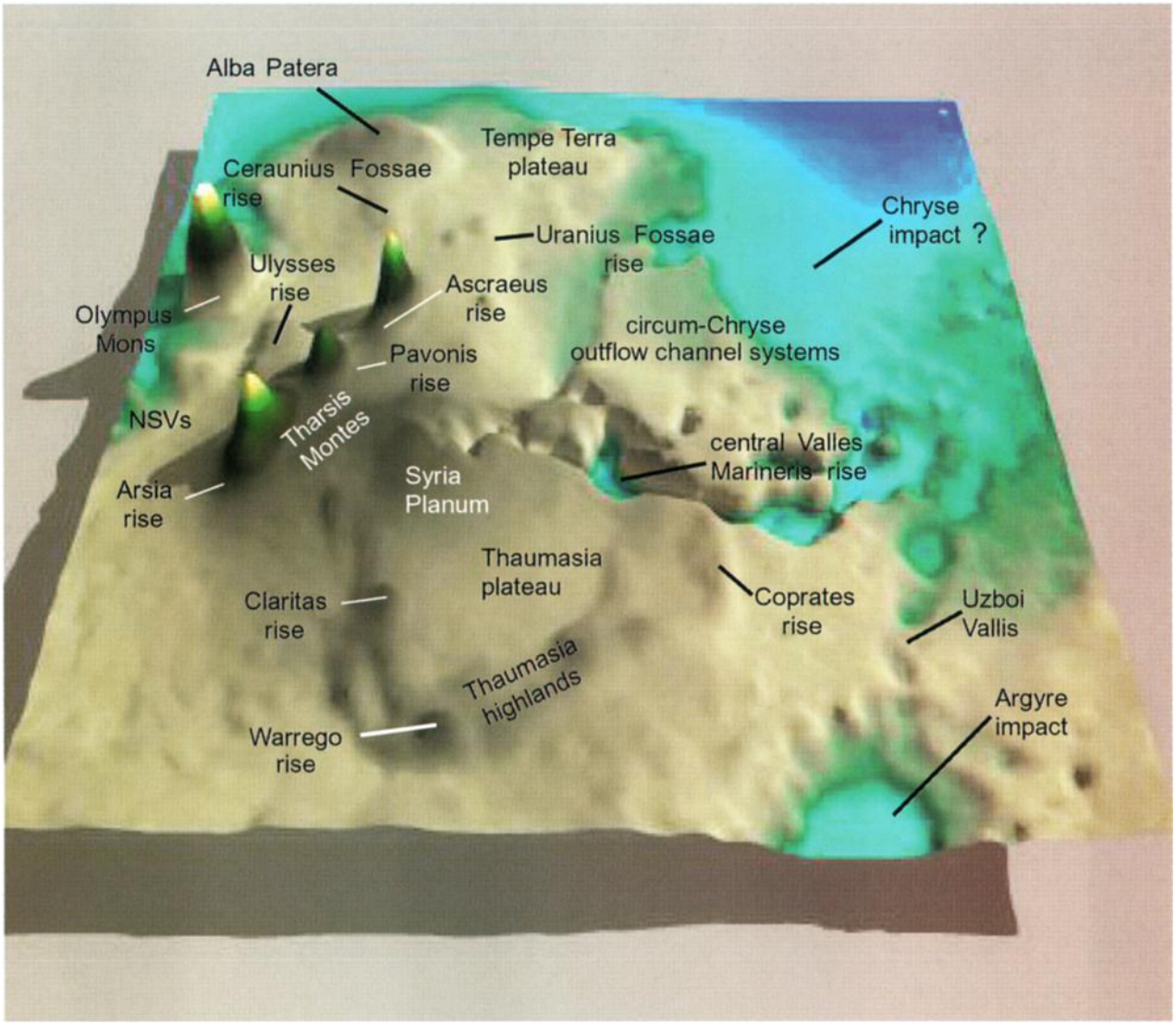

Plate 3. Three-dimensional portrayal of the major geologic features of the Tharsis Magmatic Complex using MOLA data (Stage 5, Amazonian [*Dohm and Tanaka*, 1999; *Dohm et al.*, 2001a]).

addition, materials of regional extent with no obvious point source (e.g., volcanic construct) were removed from the topographic reconstructions of earlier stages of the complex's development using published geologic map information coupled with MOLA-based geologic cross sections. For example, Early Hesperian (Stage 3) ridged material was removed from the Noachian reconstruction (Stage 1 and early part of Stage 2) using the geologic map of the western hemisphere [*Scott and Tanaka*, 1986] and MOLA-based geologic cross sections (e.g., Plates 8a–8c). In other situations, materials were added to approximate the original topography that may have been subsequently worn down by erosional processes for each stage of the TMC's development. For example, because Claritas rise developed during the Noachian Period [*Anderson et al.*, 1998, 2001] and was subsequently modified by erosional and tectonic processes, material was added to the rise to approximate its original configuration during Stage 1 (Plate 7). Again, we wish to reemphasize that this methodology is qualitative, based on experience with terrestrial and Martian geology. Although the details (e.g., unit thicknesses) will be refined as our knowledge of Mars increases, the major features and sequences of events presented here provide an improved understanding of the evolution the Tharsis Magmatic Complex as well as its influence on global geology and paleoclimate.

3. Geologic Summary of the Evolution of the Tharsis Magmatic Complex

This summary provides an interpretive geologic history of the Tharsis Magmatic Complex based on topographic, stratigraphic, paleoerosional, and paleotectonic information compiled from the work of numerous investigators. Key information used in this construction includes the spatial and temporal relations among shield volcanoes, igneous plateaus, magmatic-driven centers of tectonic activity, fault and rift systems, and lava flow fields (see Plates 1 and 2). Stage information is based on *Dohm and Tanaka* [1999] and *Dohm et al.* [2001a] and roughly corresponds to the Martian stratigraphic scheme [*Tanaka*, 1986].

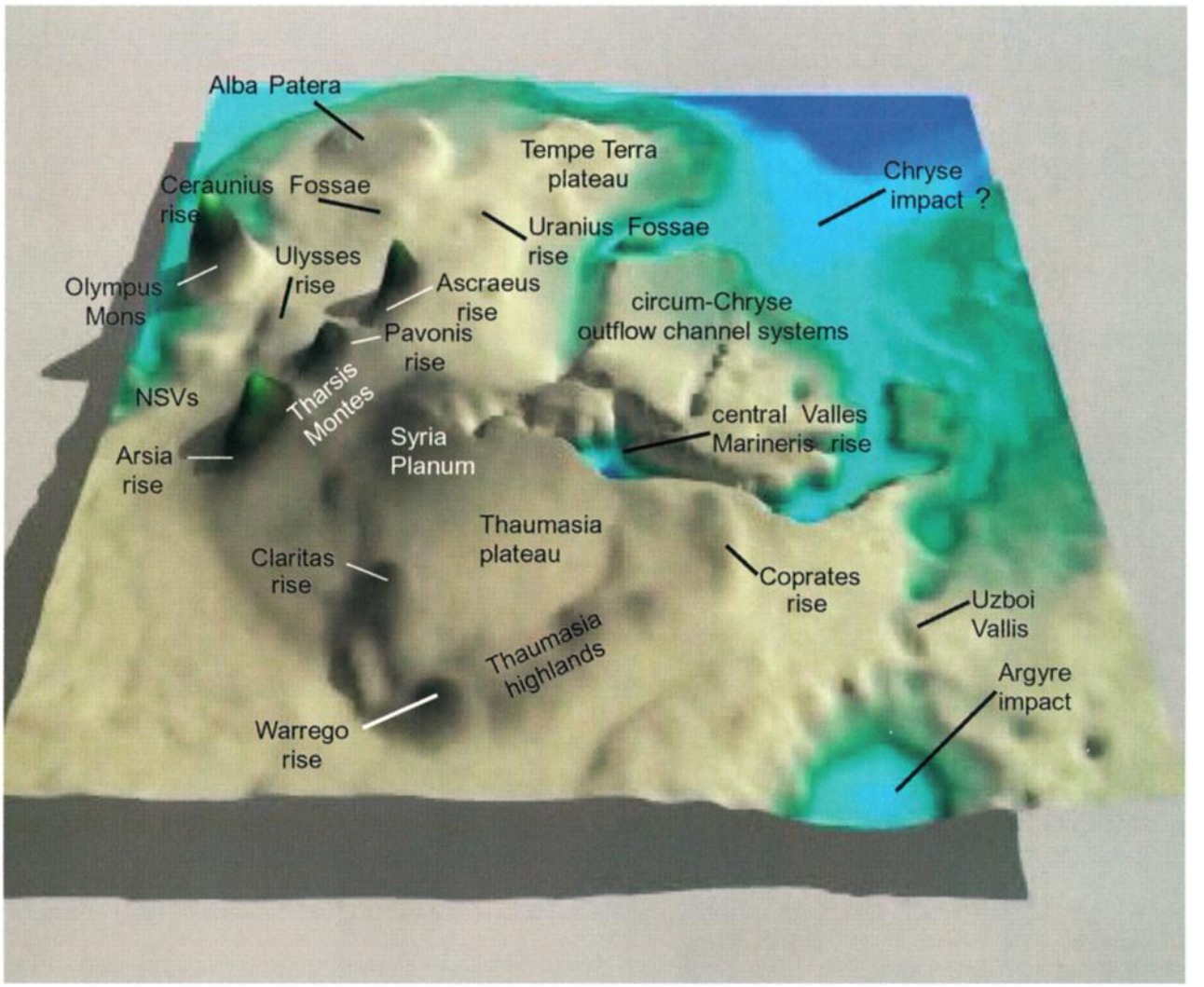

Plate 4. Three-dimensional portrayal of the major geologic features of the Tharsis Magmatic Complex during Stage 4 (Late Hesperian–Early Amazonian [*Dohm and Tanaka*, 1999; *Dohm et al.*, 2001a]). When compared to Stage 5 (Plate 3), significant highlights include (1) less developed shield volcanoes, including Olympus Mons, Tharsis Montes, and Alba Patera and their associated lava flows, (2) recession of the highland-lowland boundary, (3) less modified Thaumasia plateau (cessation of plateau uplift is mapped as Early Hesperian [*Dohm and Tanaka*, 1999; *Dohm et al.*, 2001a], and (4) less infilled and more defined basins (e.g., Chryse and Argyre) and canyons (e.g., Valles Marineris) as well as deeper outflow channels.

3.1. Early to Middle Noachian, Part of Stage 1 (Plates 1, 2, and 7)

The greatest percentage of faults preserved in Noachian materials of the western hemisphere originate near the central part of the Claritas rise. This region is marked by an enormous rift system and highly deformed promontories interpreted to be basement complex. The Claritas rise is a center of activity representing a region of broad magmatic-driven uplift and associated volcanism and tectonism. In addition to Claritas, magmatic-driven tectonic activity is also identified for the Tempe plateau and pre-Tharsis Montes rises: Uranius, Ceraunius, and Arsia SW. Uncertainty exists in the commencement of ancient local and regional centers of magmatic-related activity. Syria Planum and Arsia rise, for example, most likely began as local centers of activity during the Early to Middle Noachian with substantial growth, perhaps episodically, through the Hesperian. The Noachian magmatic activity mostly occurs along large fracture/fault zones, many of which may represent large dislocations in the Martian crust/lithosphere. Such dislocations may be the result of the TMC development and (or) represent plate or block boundaries formed during the period of high heat flow [e.g., *Schubert et al.*, 1992; *Sleep*, 1994].

Broad rises, rugged mountain ranges, and a ridge of materials, which may represent the remains of a highly eroded rim of Chryse impact basin, partly form the margin of the proposed enormous Noachian drainage basin. The development of the highland-lowland boundary sometime during the Middle to Late Noachian may have resulted in a substantially different paleohydrologic regime in Chryse Planitia region, including an enhanced hydraulic gradient.

3.2. Late Noachian to Early Hesperian, Stage 2 (Plates 1, 2, and 6)

In addition to continued growth of the Arsia rise (pre-Tharsis Montes), centers of magmatic-driven tectonic activity

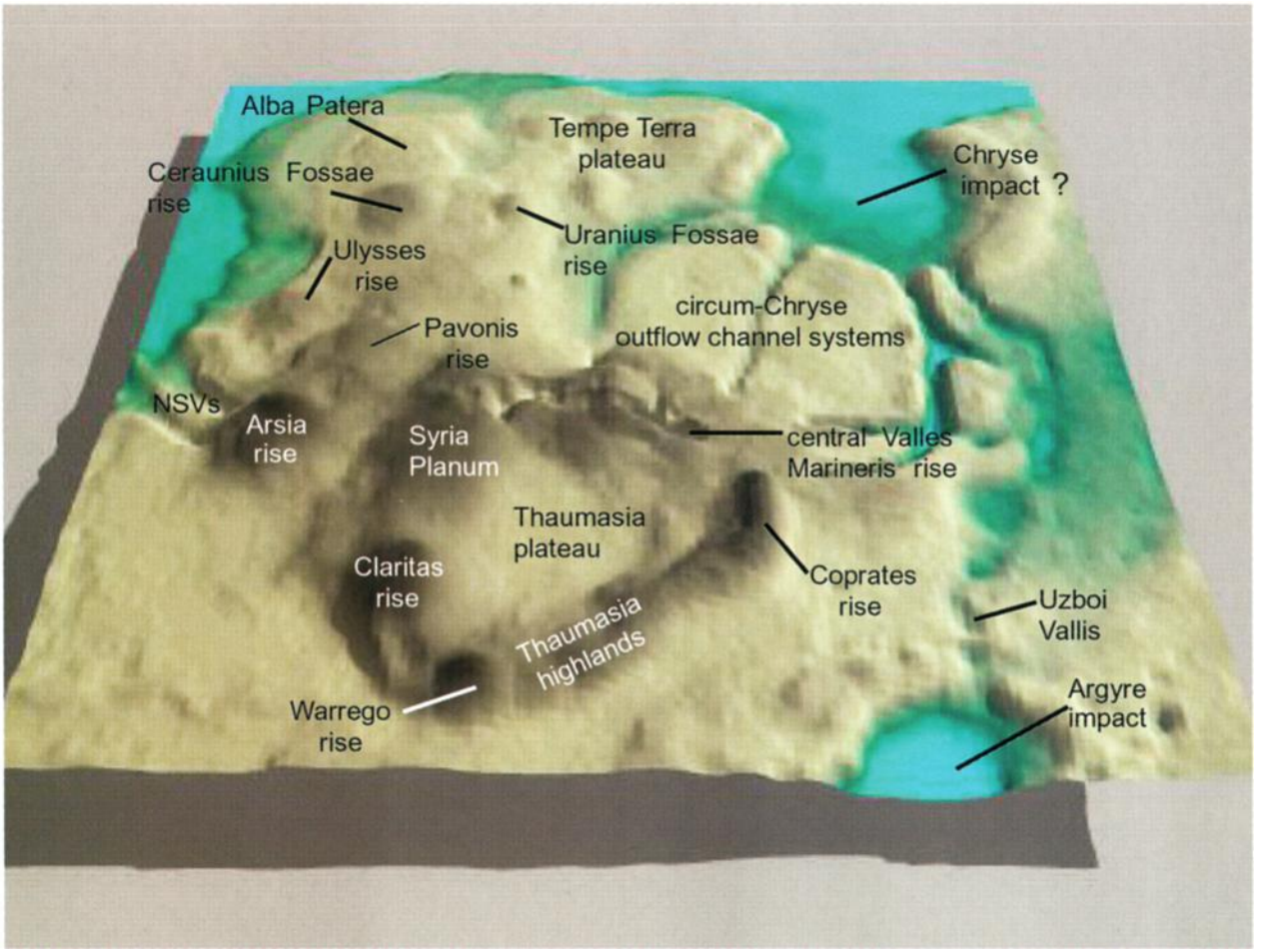

Plate 5. Three-dimensional portrayal of the major geologic features of the Tharsis Magmatic Complex during Stage 3 (Early Hesperian [*Dohm and Tanaka*, 1999; *Dohm et al.*, 2001a]). When compared to Stage 4 (Plate 4), significant highlights include (1) absence of Olympus Mons and Tharsis Montes shield volcanoes, including associated lava flows, (2) incipient Pavonis rise, (3) less developed Alba Patera and associated lava flows, (3) more prominent Syria Planum, Ceraunius Fossae, Uranius Fossae, central Valles Marineris, Arsia, Claritas, and Warrego rises and the NSVs, (4) recession of the highland-lowland boundary, (5) less modified Thaumasia (cessation of plateau uplift is mapped as Early Hesperian [*Dohm and Tanaka*, 1999; *Dohm et al.*, 2001a]) and Tempe Plateaus, and (6) less infilled and more defined basins (e.g., Solis, Chryse, and Argyre) and smaller and less defined outflow channels.

and possible associated volcanic eruptions and hydrothermal activity are identified near the central part of Valles Marineris, Syria Planum, and the source region of Warrego Valles. Numerous faults, for example, are radial to or concentric about the central part of Valles Marineris, representing a broad center of magmatic-driven uplift along a large crustal/lithospheric dislocation (Plate 9). Similar to the central part of Valles Marineris, Syria Planum is also a site of long-lived (Noachian through at least Late Hesperian) magmatic/tectonic activity, which includes domal uplift, volcanism, and associated radial and concentric faulting, but at a much larger scale and longer duration than is recognized at the central part of Valles Marineris.

Magmatic-related activity such as doming underlying Arsia Mons and at Syria Planum and central Valles Marineris may be genetically associated with the early development of the circum-Chryse outflow channel systems [e.g., *Dohm et al.*, 1998; *McKenzie and Nimmo*, 1999] as well as the formation of the newly defined northwest slope valleys [*Dohm et al.*, 2000c, 2001b], located on the opposite side of the Tharsis rise from the circum-Chryse system of outflow channels, several thousands of kilometers to the west. In addition, the source region of Warrego Valles has been interpreted to be a site of intrusive-related doming and tectonic and hydrothermal activity resulting in the formation of well-defined valley networks of Warrego Valles [*Gulick*, 1993; *Dohm and Tanaka*, 1999; *Dohm et al.*, 2001a].

The Thaumasia plateau uplift also occurred during this time [*Dohm and Tanaka*, 1999; *Dohm et al.*, 2001a]. The plateau uplift and local/regional centers of magmatic activity largely modified the paleotopography of the TMC region. These activities resulted in the modification and deformation of the Tharsis basin, releasing catastrophic floods that led to the early formation of the circum-Chryse system of outflow channels [e.g., *Rotto and Tanaka*, 1995; *Nelson and Greeley*, 1999] and the northwest slope valleys. This probably drove volatiles (e.g., groundwater) from uplifted regions such as the central part of Valles Marineris and Syria Planum into nearby topographic lows [e.g., *Dohm et al.*, 2000b; *Barlow et al.*, 2001]. The time of initial formation of these outflow channel systems is uncertain (Plate 2). For example,

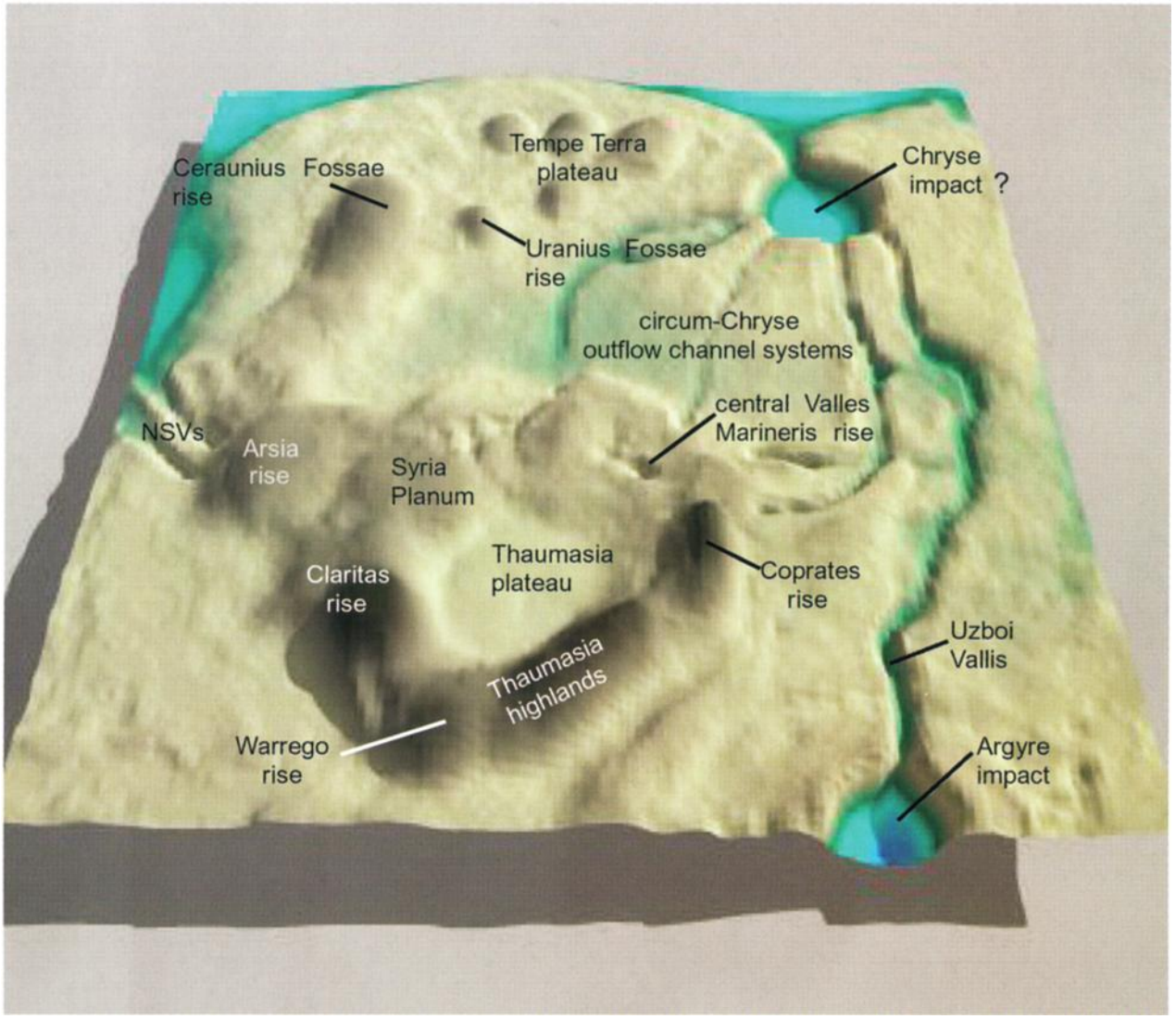

Plate 6. Three-dimensional portrayal of the major geologic features of the Tharsis Magmatic Complex during Stage 2 (Late Noachian–Early Hesperian [*Dohm and Tanaka*, 1999; *Dohm et al.*, 2001a]). When compared to Stage 3 (Plate 5), significant highlights include (1) absence of Alba Patera and associated lava flows, (2) less prominent Warrego and Arsia rises, (3) incipient trough development at Valles Marineris, (3) more prominent mountain ranges of Coprates rise and Thaumasia highlands, Tempe Terra and Thaumasia igneous plateaus, Syria Planum, Ceraunis Fossae and Claritas rises, (3) recession of the highland-lowland boundary, (4) less modified Thaumasia and Tempe plateaus, and (6) less infilled and more defined basins (e.g., Solis, Chryse, and Argyre), the NSVs, and Uzboi Vallis and smaller and less defined outflow channels.

lava flows sourcing from Stage 1 and Stage 2 centers of activity may have partly infilled and followed paleovalleys associated with early development of the large outflow channel systems, resulting in an inversion of topography (lava ridges/mesas resulting from subsequent erosion of less competent brecciated surrounding materials). Later episodes of magmatic-triggered flooding may have formed new valleys or may have followed paleovalleys. Also during this time, extensive older ridged plains materials [*Dohm and Tanaka*, 1999; *Dohm et al.*, 2001a] and intercrater materials were emplaced in topographically low areas. Some intercrater materials may be the result of phreatomagmatic explosions, such as in the Valles Marineris region, where magma–water–water ice interactions have been proposed [*Chapman and Tanaka*, 2001].

3.3. Early Hesperian, Stage 3 (Plates 1, 2, and 5)

Continued magmatic/tectonic activity is identified at Arsia-SW dome (continued growth of Tharsis rise drainage divide), Syria Planum, and Tempe plateau. Incipient activity (pre-Tharsis Montes activity) is also recognized in the Pavonis Mons [*Plescia and Saunders*, 1982; *Anderson et al.*, 1998, 2001] and Alba and Ulysses Paterae regions. Also during the Early Hesperian Period, additional development is recorded for the circum-Chryse system of outflow channels and at the north-

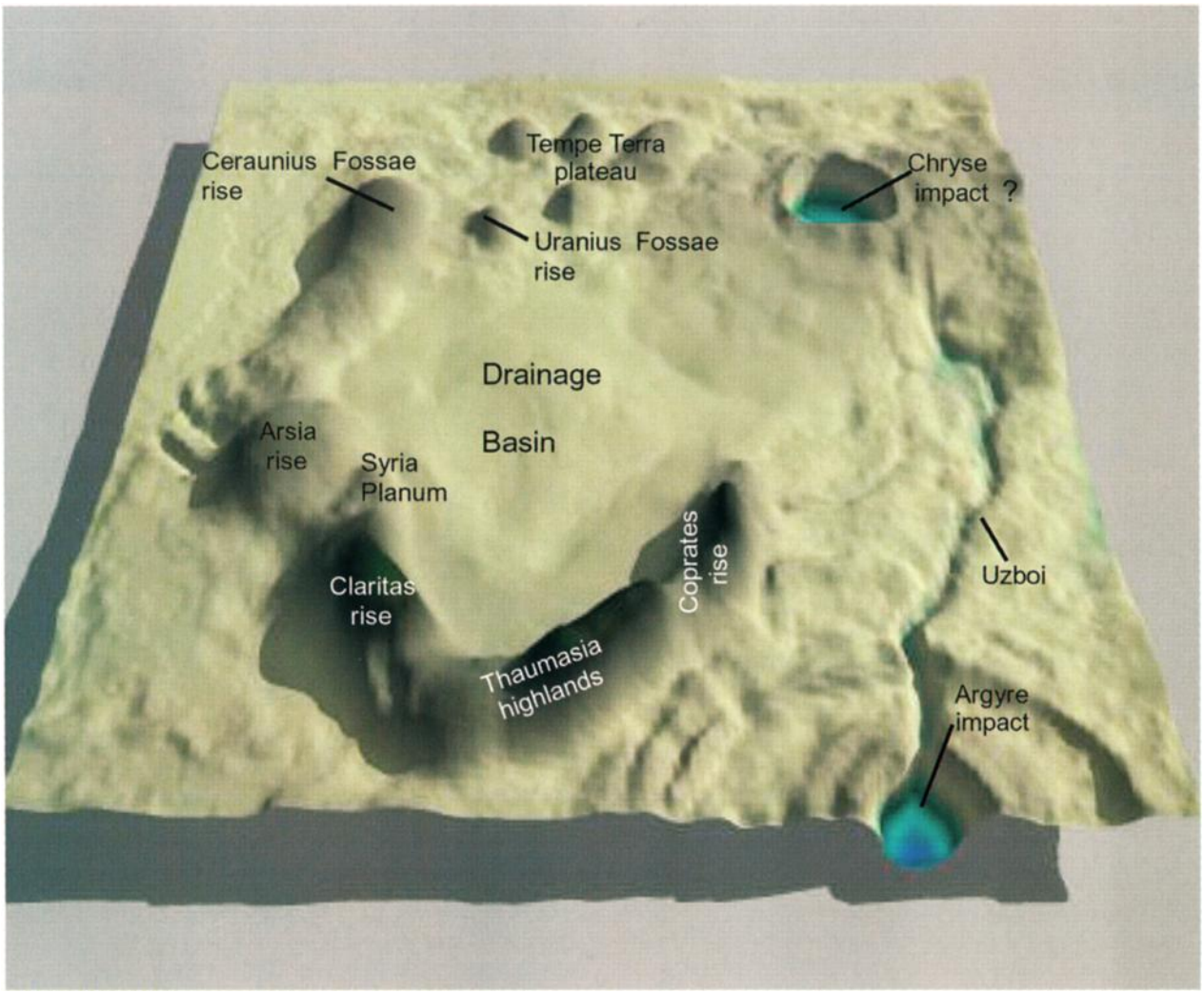

Plate 7. Three-dimensional portrayal of the major geologic features of the Tharsis Magmatic Complex [*Solomon and Head*, 2000; *Dohm et al.*, 2000b; *Anderson et al.*, 2001] during the Early to Middle Noachian Period (part of Stage 1 [*Dohm and Tanaka*, 1999; *Dohm et al.*, 2001a]), including the drainage basin. When compared to Stage 2 (Plate 6), significant highlights include (1) drainage basin, (2) narrower and sharper mountain ranges of Coprates rise, Thaumasia highlands, and multiringed structures of the Argyre impact basin (the Charitum and Nereidum Montes), (3) incipient Ceraunis Fossae, Claritas, and Arsia rises, Syria Planum, and Tempe plateau, (4) absence of highland-lowland boundary, Valles Marineris, circum-Chryse outflow channel systems, and Thaumasia plateau, (5) more distinct Argyre and putative Chryse impact basins, and (6) less distinct Uzboi Vallis.

western slope valleys, possibly related to another pulse of magmatic activity at Arsia-SW dome, Syria Planum, and the central part of Valles Marineris. Extensive younger ridged plains materials were emplaced in topographic lows.

3.4. Late Hesperian to Early Amazonian, Stage 4 (Plates 1, 2, and 4)

Significant volcanic activity is also recorded during the Late Hesperian and Early Amazonian, including the development of Olympus Mons and the Tharsis Montes shield volcanoes. Also emplaced were voluminous sheet lavas centered at the large shield volcanoes and at Syria Planum. Lava flows centered at Arsia Mons, for example, may extend to the northwest as far as the northwestern slope valleys embaying the gigantic northwest trending promontories and partly infilling the system of valleys [*Zimbelman et al.*, 2000].

A significant transition from magmatic-tectonic activity to volcanic activity is observed at the major centers of activity, notably at Syria Planum [*Dohm and Tanaka*, 1999; *Dohm et al.*, 2001a]. The final appearance of large-scale tectonism for the western hemisphere is associated with the dominant center of tectonic activity, Alba Patera [*Anderson et al.*, 1998, 2001]. Significant outflow channel formation also occurred in the circum-Chryse system of outflow channels during the Late Hesperian and into the Early Amazonian. This may be related to yet another pulse of magmatic activity at Tharsis Montes, Syria Planum, and the central part of Valles Marineris, which is consistent with the driving mechanism in the MEGAOUTFLO hypothesis [*Baker et al.*, 1991, 2000].

3.5. Amazonian, Stage 5 (Plates 1, 2, and 3)

Evidence for continued growth of Olympus Mons and the Tharsis Montes shield volcanoes is identified during this geologic period. Isolated occurrences of magmatic/tectonic activity appear to be associated with continued construction of the Tharsis Montes shield volcanoes and Olympus Mons. Other

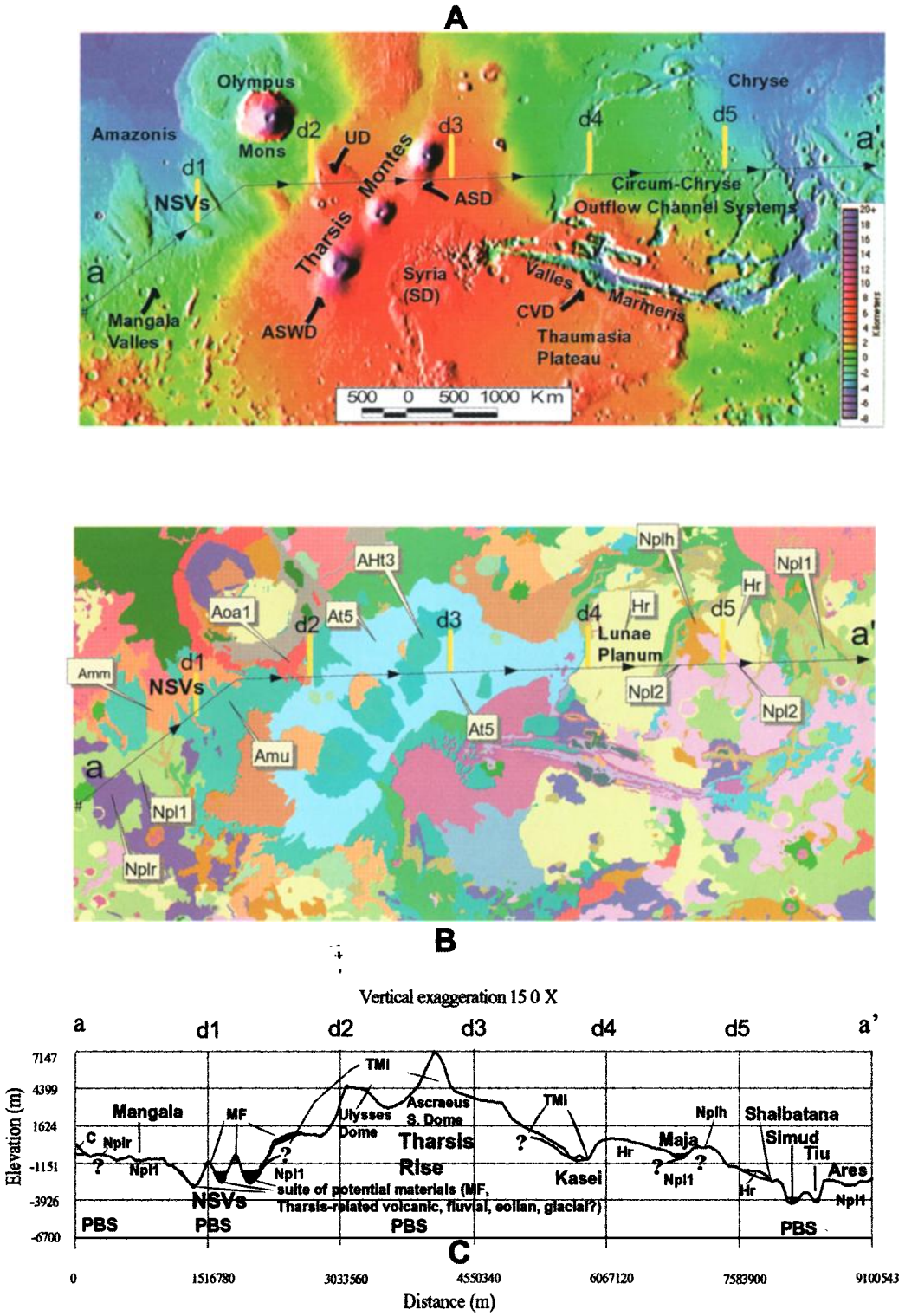

Plate 8. (a) MOLA shaded relief map showing features of interest, including NSVs, Tharsis rise, circum-Chryse outflow channel systems, and centers of tectonic activity [*Anderson et al.*, 1998; *Dohm et al.*, 1998] interpreted to represent magmatic-driven doming events (UD, Ulysses; ASD, Ascaeus south; ASWD, Arsia southwest; CVD, central Valles; SD, Syria), (b) part of the geologic map of the western equatorial region of Mars (representative map units are shown [*Scott and Tanaka*, 1986]), (c) generalized geologic cross section (a-a′, transect of A and B; PBS, potential location of basement structures; TMl, Tharsis Montes lavas; MF, Medusae Fossae materials) [*Dohm et al.*, 2001b, Figure 2].

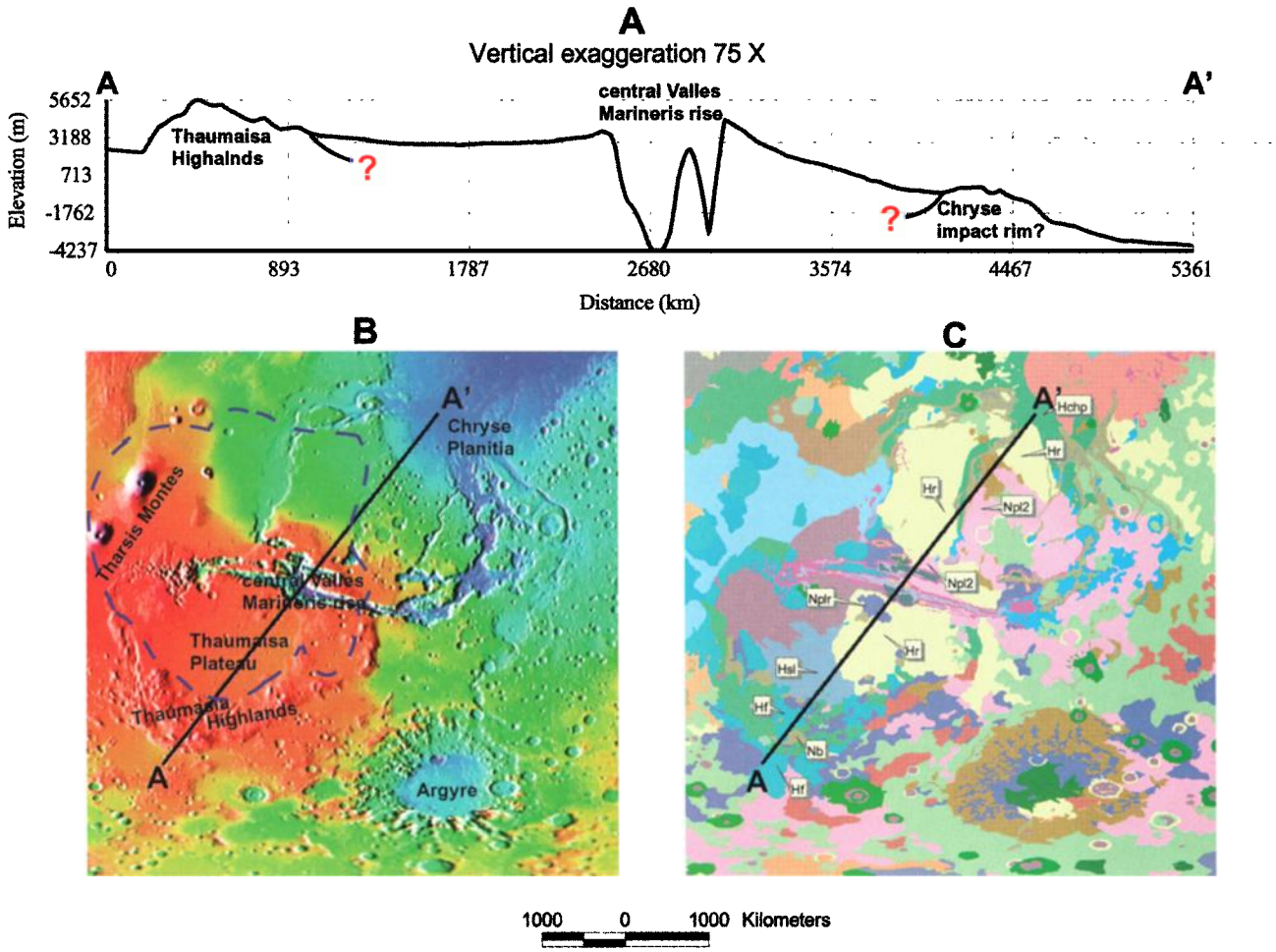

Plate 9. (a) Present-day MOLA profile (transect A-A′) across the west central part of the Thaumasia highlands, the southeast part of the Noachian drainage basin (queried blue line represents uncertain basin extent), including the central Valles Marineris rise (center of tectonic activity, interpreted to be the result of magmatic-driven uplift [*Dohm et al.*, 1998; *Anderson et al.*, 1998, 2001; *Dohm et al.*, 2000b]), and materials of inferred rim of Chryse impact basin, (b) MOLA shaded relief map showing features of interest, including the approximated boundary of the Noachian drainage basin (dashed blue line) and the central Valles Marineris rise, and (c) part of the geologic map of the western equatorial region of Mars (representative map units are shown [*Scott and Tanaka*, 1986]).

than minor graben formation associated with the final stages of Alba Patera, these local volcanic sources may represent late-stage pulses of magmatic/tectonic activity in the Tharsis region.

4. Basin Model: Physiographic Setting and Stratigraphic Summary

During the Early to Middle Noachian (early part of Stage 1), topographic highs associated with centers of tectonic activity (Uranius Fossae, Ceranius Fossae, Arsia and Claritas rises), rugged mountain ranges of the east trending Thaumasia highlands and north trending Coprates rise, high-standing terrain located southwest of Chryse Planitia (interpreted here to be a highly eroded impact crater rim), and Tempe plateau formed the margins of the proposed drainage basin (Plate 7). During this same time period, lavas, sediments, and volatiles partly infilled the basin, resulting in a large aquifer system. The partial infilling of the basin perhaps coincides with reported higher rates of planetwide surface degradation than for post-Noachian time [*Masursky et al.*, 1977; *Pieri*, 1980; *Barlow*, 1990; *Craddock and Maxwell*, 1993; *Scott et al.*, 1995; *Carr and Chuang*, 1997; *Tanaka et al.*, 1998].

The basin/aquifer system was subsequently obscured and deformed by middle Noachian and younger geologic activity (Stages 1–5), including (1) the Thaumasia plateau uplift, (2) continued growth of the Arsia rise and the development of other centers of tectonic activity, which also correspond to topographic rises (including central Valles Marineris rise, Syria Planum, and pre-Tharsis Montes Pavonis), (3) the emplacement of the intercrater plains materials, older and younger ridged plains materials, and lavas associated with Syria Planum and Tharsis Montes and local sources such as fissure fed lavas, and (4) the construction of the Tharsis Montes shield volcanoes. The interaction of magmatic intrusions with water-bearing strata may have resulted in lateral migration of subsurface volatiles away from magmatic-driven heating and

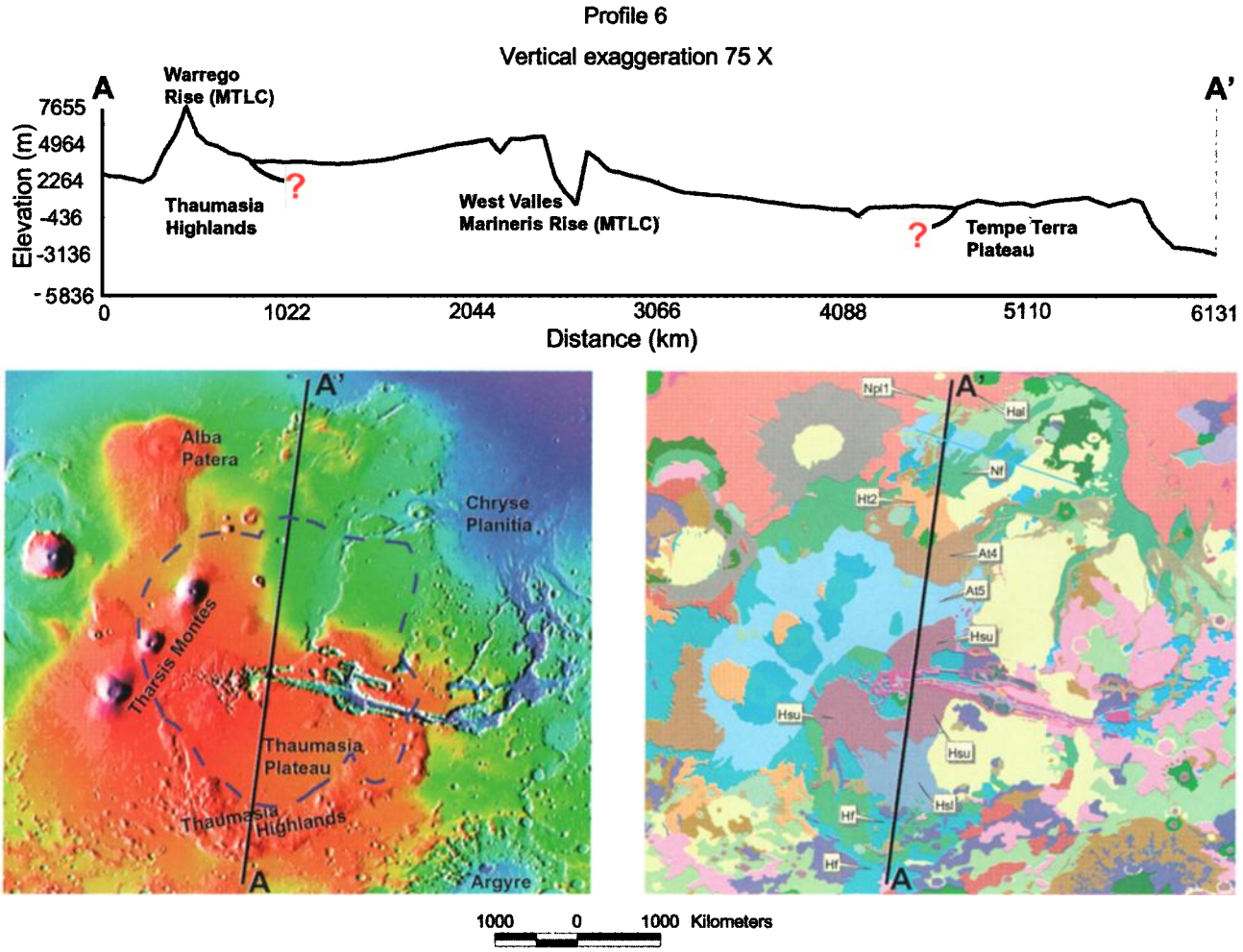

Plate 10. (a) Present-day MOLA profile (transect A-A′) across the Warrego rise (center of tectonic activity, interpreted to be the result of magmatic-driven uplift [*Anderson et al.*, 1998, 2001; *Dohm et al.*, 1998; *Dohm and Tanaka*, 1999; *Dohm et al.*, 2000b, 2001a]), west central part of Thaumasia highlands, central part of the Noachian drainage basin (queried blue line represents uncertain basin extent), including west central Valles Marineris rise (center of tectonic activity, interpreted to be the result of magmatic-driven uplift [*Anderson et al.*, 1998, 2001; *Dohm et al.*, 1998; *Dohm and Tanaka*, 1999; *Dohm et al.*, 2000b, 2001a]), and Tempe Terra plateau, (b) MOLA shaded relief map showing features of interest, including the approximated boundary of the Noachian drainage basin (dashed blue line) and the west central Valles Marineris rise, and (c) part of the geologic map of the western equatorial region of Mars (representative map units are shown [*Scott and Tanaka*, 1986]).

uplift. Such occurrences were probably common throughout the evolution of the drainage basin [*Anderson et al.*, 1998, 2001; *Dohm et al.*, 1998, 2000e; *Solomon and Head*, 2000] and may explain the concentrations of near-surface volatiles in the Solis Planum region expressed by an anomalous concentration of layered ejecta craters [*Barlow et al.*, 2001]. In addition, stacked sequences of basin materials were locally exposed in the canyon walls of Valles Marineris by magmatic-driven doming, tectonic deformation, and erosion.

Whether the proposed drainage basin is strictly the result of surrounding topographic highs or whether there is an endogenic component is difficult to answer. As noted in the previous section, the central part of the proposed basin, Valles Marineris, is the location of centers of tectonic activity. These centers are interpreted to be the result of magmatic-driven uplifts and local volcanism, dike emplacement, and hydrothermal activity. In addition, more than half of the proposed basin was modified by the Thaumasia plateau uplift, which may have been the result of magma plume head. Such activity may be likened to topographic inversions observed on Earth. Large igneous plateaus occur on both continental and oceanic crust in purely intraplate settings, on present and former plate boundaries (large lithospheric weaknesses), and along the edges of continents and are interpreted to be the result of plume activity [*Coffin and Eldholm*, 1994]. The largest terrestrial example of plume-derived igneous plateau growth among topographic basins is Ontong-Java Plateau in the west central Pacific [*Richardson et al.*, 2000].

5. Aquifer Characteristics

The sources of the largest Martian outflow channel systems (circum-Chryse and the proposed northwestern slope valleys (NSVs)) suggest that the infill materials of the gigantic drain-

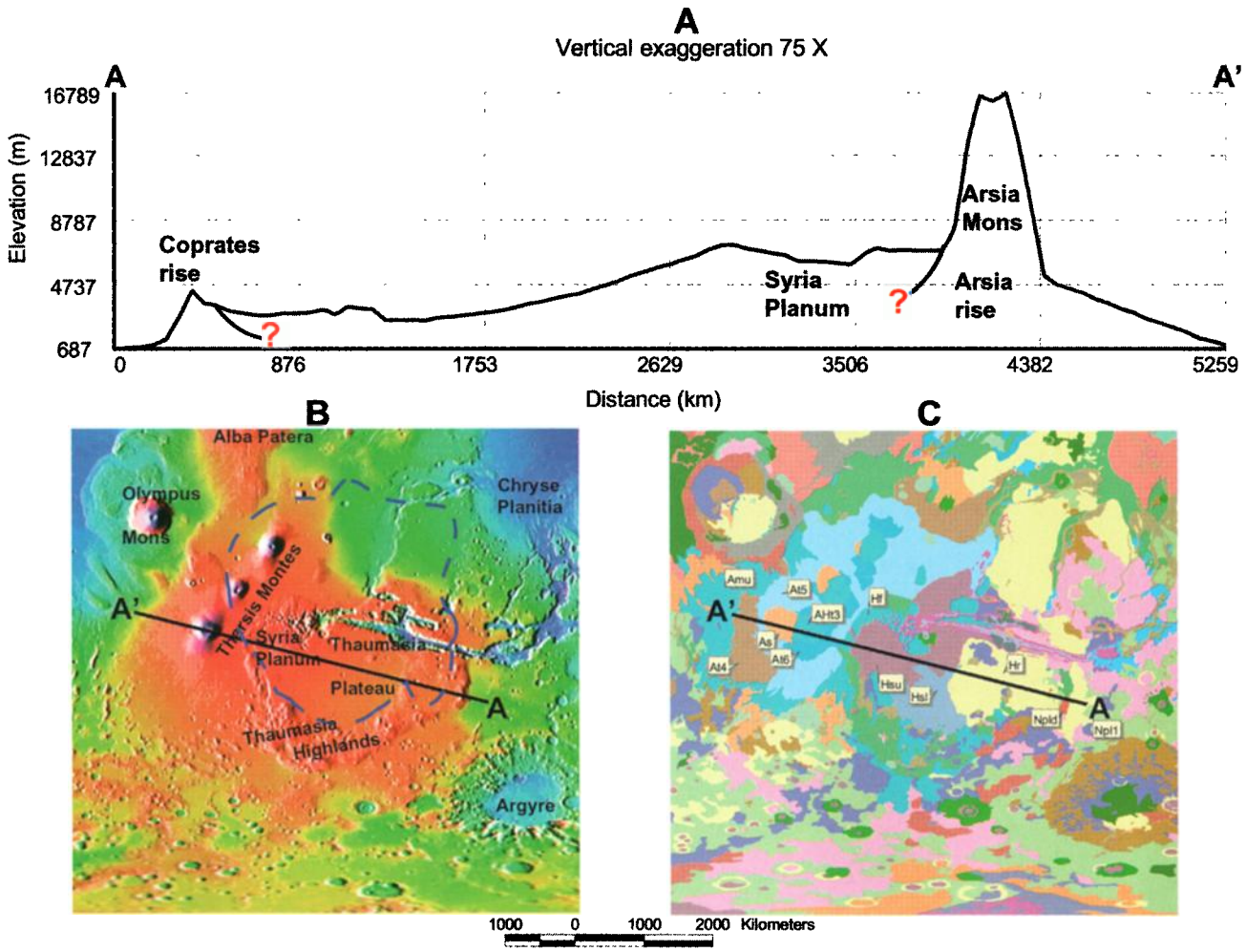

Plate 11. (a) Present-day MOLA profile (transect A-A′) across the Coprates rise [*Schultz and Tanaka*, 1994; *Dohm and Tanaka*, 1999; *Dohm et al.*, 2001a], southern part of the Noachian drainage basin (queried blue line represents uncertain basin extent), Syria Planum (center of tectonic activity, interpreted to be the result of magmatic-driven uplift and volcanism [*Tanaka and Davis*, 1988; *Anderson et al.*, 1998, 2001; *Dohm et al.*, 1998; *Dohm and Tanaka*, 1999; *Dohm et al.*, 2000b, 2001a]), Arsia rise (center of tectonic activity, interpreted to be the result of magmatic-driven uplift and volcanism [*Anderson et al.*, 1998, 2001; *Dohm et al.*, 2000b]), and Arsia Mons [*Scott and Tanaka*, 1986; *Scott and Zimbelman*, 1995], (b) MOLA shaded relief map showing features of interest, including the approximated boundary of the Noachian drainage basin (dashed blue line), and (c) part of the geologic map of the western equatorial region of Mars (representative map units are shown [*Scott and Tanaka*, 1986]).

age basin may have produced a highly productive aquifer. Large pulses of magmatic activity related to the development of the Tharsis magmatic complex [*Dohm et al.*, 2000a, 2000b] probably resulted in the partial infilling of the basin by emplacing stacked sequences of lavas. Evidence of this may be the layered walls of Valles Marineris, which have been interpreted to consist of flood lavas [e.g., *Witbeck et al.*, 1991; *Lucchitta et al.*, 1992]. Depending on Noachian climate conditions, these sequences may be interfingered with lacustrine and/or eolian deposits. Furthermore, the basaltic sequences are highly fractured by magmatic and tectonic activities [e.g., *Scott and Tanaka*, 1986; *Tanaka and Davis*, 1988; *Tanaka*, 1990; *Scott and Dohm*, 1990a, 1990b, 1997; *Anderson et al.*, 1998, 2001; *Dohm et al.*, 1998, 2000b; *Dohm and Tanaka*, 1999; *Solomon and Head*, 2000; *Dohm et al.*, 2001a]. Highly fractured basalt can have unusually high values of hydraulic conductivity in terrestrial aquifers. Preliminary analyses of the equations that govern subsurface hydrological behavior imply not only that this relationship remains true for a Martian aquifer but that the value of hydrologic conductivity may be amplified owing to the lowered frictional resistance afforded by the lesser gravity of Mars [*Dohm et al.*, 2000c, 2001b]. Additionally, any interfingered sedimentary deposits would serve as local reservoirs for subsurface water capable of being tapped by the highly fractured basalts.

We estimate the average depth of the Tharsis basin to be between 2 and 7 km (for example, Plates 9–11). The measured area of the basin is approximately 9×10^6 km^2 (Plates 1, 7, 9–11), and as such, the fill volume for an average depth of 5 km is approximately 4.5×10^7 km^3. If the fill were largely composed of highly fractured vesicular extrusive basalts, then the porosity and permeability would be very high. On Earth the

porosity of unfractured vesicular basalts ranges from roughly 20% for low vesicularity to roughly 75% for highly vesicular scoriaceous basalts [*Saar and Manga*, 1999]. The porosity and especially the permeability could be even higher in the Tharsis region, as they are highly fractured from tectonic processes, including faulting. Unlike the highly fractured surfaces that prevail throughout the Tharsis Magmatic Complex and thus high potential permeabilities, impact crater events may lower porosity and permeability because they will produce fines that infill pore spaces [*MacKinnon and Tanaka*, 1989]. When compared to highly cratered surfaces of the southern highlands, however, the proposed basin region (also of the southern highlands) is significantly less cratered.

If the terrestrial porosities are characteristic of the Tharsis basin fill, then the potential volume of water contained in the aquifer would be more than equivalent to the volume of water required to create the putative ocean in the northern plains estimated at 1.4×10^7 km^3 [*Head et al.*, 1999]. For example, if the porosity of basalts was 44%, and the removal of total water from the aquifer was 60%, the minimum fill volume of the northern plains ocean would be achieved. The inferred porosity is well within the values measured for unfractured basalt flows of moderate porosity [*Saar and Manga*, 1999]. We realize, however, that it is hard to imagine that 60% of the entire aquifer could have been discharged in one event. In addition, one can only guess at the effectiveness of the proposed aquifer system. Thus we pose the following considerations. Other hydrogeologic activities associated with catastrophic flooding and related short-lived ($\sim 10^4$ to 10^5 year) episodes of quasi-stable climatic conditions [*Baker et al.*, 1991, 2000] may have also contributed water to the hypothesized oceans by mechanisms such as spring-fed activity along areas of the highland-lowland boundary. Certainly, other aquifers may have contributed to the putative northern plains ocean as well, especially following catastrophic flood events and related short-lived climatic perturbations described by Baker et al. In addition, a large quantity of ground ice (e.g., stagnant ice sheets) may have already been in place in the northern plains during the period(s) of catastrophic flooding [*Dohm et al.*, 2000c, 2001b]. This large quantity of ice would be the likely consequence of an earlier warm and wet phase of Mars, possibly induced by catastrophic flooding [*Baker et al.*, 1991, 2000]. As new floodwaters washed over the northern plains, the additional heat would melt the upper layers of ice, and the gradients created would allow the melt water to cycle into the hydrologic system. Alternatively, a proposed massive debris-flow ocean [*Tanaka et al.*, 2001] and/or a mud ocean [*Jöns*, 1986] require less source water then a putative vast northern ocean [*Parker et al.*, 1987, 1993; *Head et al.*, 1999]. In addition, potential paleolakes, which also require less source water, have been mapped in the northern plains [*Scott et al.*, 1995].

6. Discussion

There are several significant observations/characteristics in the Tharsis and surrounding regions that might be collectively explained by an Early to Middle Noachian drainage basin. These include (1) the paucity of Noachian outcrops (Plates 8–11) [e.g., *Scott and Tanaka*, 1986; *Rotto and Tanaka*, 1995; *Dohm and Tanaka*, 1999; *Nelson and Greeley*, 1999; *Dohm et al.*, 2001a] and crustal magnetic anomalies in the proposed basin region [*Acuna et al.*, 1999], (2) a sufficient source of water necessary to carve the circum-Chryse outflow channel systems and the recently proposed structurally controlled system of valleys that routed Noachian and Early Hesperian floods from the Arsia Mons region to the northwest into Amazonis Planitia [*Dohm et al.*, 2000c, 2001b]), (3) the thick sequences of layered materials exposed in the walls of Valles Marineris by magmatic, tectonic, and erosional activity [*Scott and Tanaka*, 1986; *Witbeck et al.*, 1991; *Lucchitta et al.*, 1992; *Dohm et al.*, 1998; *McKenzie and Nimmo*, 1999; *McEwen et al.*, 1999; *Dohm et al.*, 2001a], (4) an anomalous concentration of layered ejecta craters in the Solis and Thaumasia Planae regions [*Barlow et al.*, 2001], (5) the volatile-rich nature of Valles Marineris [*Scott and Tanaka*, 1986; *Witbeck et al.*, 1991; *Lucchitta et al.*, 1992], and (6) the observed hematite deposits detected in Valles Marineris [*Christensen et al.*, 1998; *Noreen et al.*, 2000].

The thick sequence of layered materials observed in the canyon walls of Valles Marineris, for example, may represent the accumulation of volcanic and other types of materials shed into the basin. In addition, the hematite deposits detected in the Valles Marineris region by the Thermal Emission Spectrometer (TES) instrument may be the result of phreatomagmatic mixing between magma and groundwater or surface water within the basin [*Noreen et al.*, 2000; *Chapman and Lucchitta*, 2000]. Although the true hydrogeologic complexity of the basin and aquifer system undoubtedly eludes us, the circum-Chryse catastrophic outflow channels and the NSVs demonstrate the tremendous productivity of this Noachian aquifer. Likewise, the hypothesis that the circum-Chryse catastrophic outflow channels and northwestern slope valleys resulted from catastrophic flood events is strengthened by the identification of the gigantic drainage basin/aquifer system, a potential source for the tremendous amount of water required to sculpt the surface. The source region for catastrophic flooding generally has been thought to be the cratered highlands, which are marked by canyon systems of Valles Marineris, lava flows, and chaotic terrain [*Scott and Tanaka*, 1986; *Witbeck et al.*, 1991; *Lucchitta et al.*, 1992]. However, the magnitude and location of the most significant Martian flood features in the Tharsis region can be best explained by the existence of a Tharsis basin that facilitated the collection of large amounts of volatiles early in Martian history [*Masursky et al.*, 1977; *Pieri*, 1980; *Craddock and Maxwell*, 1993; *Scott et al.*, 1995; *Carr and Chaung*, 1997; *Tanaka et al.*, 1998]. In addition, the magmatic-triggered floodwaters that originated from the basin probably represent a major source for bodies of water in the northern plains, including oceans and paleolakes that may have resulted in short-lived climatic perturbations [*Baker et al.*, 1991, 2000].

Magmatic-driven uplifts associated with the development of the Tharsis magmatic complex subsequently transferred groundwater laterally along structurally controlled conduits within and outside of the basin. This magmatic-driven activity eventually forced some of the volatiles out of the basin by catastrophic flooding [*Baker et al.*, 1991, 2000]. Such lateral movements of volatiles throughout geologic history would result in parts of the TMC being volatile-rich and volatile-poor. Impact crater studies have revealed a region in the Solis and Thaumasia Planae (located south of Valles Marineris in the south central part of the basin; Plate 1) where an anomalous concentration of craters displaying multiple-layer ejecta morphologies is correlated with a large area of smaller onset diameters for craters displaying single-layer morphologies [*Barlow et al.*, 2001]. *Barlow et al.* [2001] proposed that the anomalous concentration marks a region that was particularly rich in volatiles (ice near the surface and liquid at greater

depths) at the time of cratering compared to other parts of the Tharsis magmatic complex and the rest of the equatorial region. Thus the impact cratering record may be consistent with a scenario where magmatic-driven uplifts locally deformed the basin, driving some of the water from the basin by catastrophic flooding and transferring volatiles from the uplifted localities into portions of the existing subsurface reservoir. This, in turn, may have resulted in a local increase of the hydraulic head. Such a linkage of processes is a predictable consequence of the interaction of magmatic intrusions and the water-bearing strata, which we envisioned to have been a common occurrence throughout the long and complex evolution of the TMC and the enormous Noachian drainage basin.

7. Alternative Models

The basin model is not the only model that offers explanations for some of the significant characteristics of the Tharsis and surrounding regions, including the putative local presence of near-surface water in the Tharsis region. A model proposed by *Clifford* [1993] also predicts near-surface water. Clifford proposed that if the planetary inventory of outgassed H_2O exceeded the pore volume of the cryosphere by more than a few percent, a subpermafrost groundwater system of global extent would necessarily result. This interconnected global aquifer allows the downward migration of polar basal melt to result in the upward migration of water at temperate and equatorial latitudes. Theoretically, this would result in the water that was lost from the crust at these latitudes by sublimation, impact, or catastrophic floods to be replenished. Although Clifford's model can adequately explain the occurrence of near-surface water in the Tharsis and surrounding regions, it cannot by itself explain the suite of significant observations and characteristics previously discussed.

The putative presence of local near-surface water in the Tharsis region, as identified by anomalous concentrations of layered ejecta craters in the Solis and Thaumasia Planae regions, can be explained by other means. A warmer and wetter climate possibly induced from the early (e.g., early to Middle Noachian) development of the Tharsis rise [*Golombek et al.*, 2000], for example, may have resulted in the ponding of water into local depressions and infiltration of water into the subsurface as it flowed across the planet's surface. As this water moved through the subsurface, it may have encountered lenses of material that prevented its downward migration, or it may have migrated in the subsurface along the natural gradient formed by the Tharsis rise. In the former case the aquitards would have led to the creation of perched aquifers. Over time these perched aquifers may have risen to the near surface or surface. As the Martian climate cooled, these near-surface aquifers would have been frozen as interstitial ice. As long as they remained frozen, they would remain trapped there, regardless of the changing gradients caused by the continued development of the Tharsis bulge. This water would be released only by the energy associated with meteoric impact [*Newsom*, 1980], resulting in the anomalous characteristics of impact craters in Solis and Thaumasia Planae. However, this model cannot explain the gigantic quantities of water required to carve the outflow channels.

There is yet another model that might explain the near-surface presence of water among other characteristics. During the early rise of Tharsis [e.g., *Banerdt et al.*, 1992; *Golombek et al.*, 2000], for example, certain topographic irregularities may have formed owing to local and regional volcanic constructs. Further assuming that the topographic irregularities formed early enough in the development of the Tharsis rise that they existed within an early warmer and wetter Martian environment [e.g., *Masursky et al.*, 1977; *Pieri*, 1980; *Golombek et al.*, 2000], the topographic irregularities would have allowed for the trapping of rainfall and runoff within localized topographic depressions. As the ponded water infiltrated into the ground, it may have become trapped near the surface as the climate cooled. If it remained frozen, it would remain in situ as Tharsis continued to rise, only to be released upon meteorite impact to produce the anomalous field of layered ejecta craters. A problem with this hypothesis, however, is that geologic mapping has not revealed any Early to Middle Noachian-age volcanic edifices within the basin region, with the exception of incipient Syria Planum [e.g., *Dohm and Tanaka*, 1999; *Dohm et al.*, 2001a].

Finally, another model to consider is one presented by *Tanaka et al.* [2000] in which Syria-Planum-centered fold and thrust structures and a cryosphere perhaps a kilometer or so thick resulted in a huge, largely sealed aquifer system within the Thaumasia plateau. Although a belt of such structures has been recognized centered about Syria Planum [*Schultz and Tanaka*, 1994], especially in the Thuamasia region [*Dohm and Tanaka*, 1999; *Dohm et al.*, 2001a], a continuous belt within the Thaumasia plateau is not observed in the stratigraphic and paleotectonic records, especially on the northern and western margins of the plateau [*Dohm and Tanaka*, 1999; *Dohm et al.*, 2001a; *Anderson et al.*, 2001]. In addition, numerous basement structures, which are radial about the Tharsis rise, form potential conduits for the migration of groundwater away from the rise. Thus the model presented by *Tanaka et al.* [2000] is not by itself sufficient to explain the suite of significant observations/characteristics discussed earlier. Thrust structures, such as those potentially observed in the Coprates rise and Thaumasia highlands regions [*Schultz and Tanaka*, 1994; *Dohm and Tanaka*, 1999], however, could have played a role in forming a highly productive Noachian drainage basin/aquifer system.

8. Conclusion

Paleotopographic reconstructions based on analyses of synthesized stratigraphic, paleotectonic, erosional, and MOLA-derived topographic map data reveal the potential existence of an enormous drainage basin in the Tharsis region during the Early to Middle Noachian period. Lavas and sediments partly infilled the basin, resulting in a highly productive regional aquifer. The stacked sequences of basin materials were subsequently exposed in the canyon walls of Valles Marineris by magmatic-driven doming, tectonic deformation, and erosion. The basin model may collectively explain (1) the paucity of Noachian outcrops and crustal magnetic anomalies in the proposed basin region, (2) the thick sequences of layered materials exposed in the walls of Valles Marineris, (3) an anomalous concentration of layered ejecta craters in the Solis and Thaumasia Planae regions, (4) the volatile-rich nature of Valles Marineris, and (5) the observed hematite deposits detected in Valles Marineris. The basin may also provide a sufficient source of water necessary to carve the circum-Chryse outflow channel systems and the recently proposed northwestern slope valleys and to form Hesperian and younger putative ocean(s) and (or) paleolakes.

Acknowledgment. In memory of a geologist, D. H. Scott. This work was supported by the National Aeronautics and Space Administration through grants to the University of Arizona.

References

Acuna, M. H., et al., Global distribution of crustal magnetization discovered by the Mars Global Surveyor MAG/ER experiment, *Science*, *284*, 790–793, 1999.

Anderson, R. C., and J. M. Dohm, Magmatic-tectonic evolution of Tharsis, *Lunar Planet. Sci.* [CD-ROM], *XXXI*, abstract 1607, 2000.

Anderson, R. C., M. P. Golombek, B. J. Franklin, K. L. Tanaka, J. M. Dohm, J. H. Lias, and B. Peer, Centers of tectonic activity through time for the western hemisphere of Mars, *Lunar Planet. Sci.* [CD-ROM], *XXIX*, abstract 1881, 1998.

Anderson, R. C., J. M. Dohm, M. P. Golombek, A. Haldemann, B. J. Franklin, K. L. Tanaka, J. Lias, and B. Peer, Primary centers and secondary concentrations of tectonic activity through time for the western hemisphere of Mars, *J. Geophys. Res.*, *106*, 20,563–20,585, 2001.

Anderson, S., and R. E. Grimm, Rift processes at the Valles Marineris, Mars: Constraints from gravity on necking and rate-dependent strength evolution, *J. Geophys. Res.*, *103*, 11,113–11,124, 1998.

Baker, V. R., Water and the Martian landscape, *Nature*, *412*, 228–236, 2001.

Baker, V. R., and D. J. Milton, Erosion by catastrophic floods on Mars and Earth, *Icarus*, *23*, 27–41, 1974.

Baker, V. R., R. G. Strom, V. C. Gulick, J. S. Kargel, G. Komatsu, and V. S. Kale, Ancient oceans, ice sheets and the hydrological cycle on Mars, *Nature*, *352*, 589–594, 1991.

Baker, V. R., R. G. Strom, J. M. Dohm, V. C. Gulick, J. S. Kargel, G. Komatsu, G. G. Ori, and J. W. Rice Jr., Mars' Oceanus Borealis, ancient glaciers, and the MEGAOUTFLO hypothesis, *Lunar Planet. Sci.* [CD-ROM], *XXXI*, abstract 1863, 2000.

Banerdt, W. B., M. P. Golombek, and K. L. Tanaka, Stress and tectonics on Mars, in *Mars*, edited by H. H. Kieffer et al., pp. 249–297, Univ. of Ariz. Press, Tucson, 1992.

Barlow, N. G., Constraints on early events in Martian history as derived from the cratering record, *J. Geophys. Res.*, *95*, 14,191–14,201, 1990.

Barlow, N. G., J. Koroshetz, and J. M. Dohm, Variations in the onset diameter for Martian layered ejecta morphologies and their implications for subsurface volatile reservoirs, *Geophys. Res. Lett.*, *28*(16), 3095–3099, 2001.

Carr, M. H., and F. C. Chuang, Martian drainage densities, *J. Geophys. Res.*, *102*, 9145–9152, 1997.

Chapman, M. G., and B. K. Lucchitta, New Mars data suggest Melas Chasma interior deposits are sub-ice volcanoes, *Geol. Soc. Am. Abstr. Programs*, *50817*, 2000.

Chapman, M. G., and K. L. Tanaka, Geologic maps of the MTM 25062 quadrangle (digital compilation) and the MTM 25067 quadrangle (manual compilation), Kasei Valles region of Mars, *U.S. Geol. Surv. Misc. Invest. Ser., Map I-2398*, scale 1:500,000, 1996.

Chapman, M. G., and K. L. Tanaka, Interior trough deposits on Mars: Subice volcanoes?, *J. Geophys. Res.*, *106*, 10,087–10,100, 2001.

Chapman, M. G., H. Masursky, and D. H. Scott, Geologic map of science study area 2, north Kasei Valles, Mars (MTM 25072 quadrangle), *U.S. Geol. Surv. Misc. Invest. Ser., Map I-2107*, scale 1:500,000, 1991.

Christensen, P. R., et al., Results from the Mars Global Surveyor Thermal Emission Spectrometer, *Science*, *279*, 1692–1697, 1998.

Clifford, S. M., A model for the hydrologic and climate behavior of water on Mars, *J. Geophys. Res.*, *98*, 10,973–11,016, 1993.

Coffin, M. F., and O. Eldholm, Large igneous provinces: Crustal structure, dimensions, and external consequences, *Rev. Geophys.*, *32*, 11–36, 1994.

Craddock, R. A., and T. A. Maxwell, Geomorphic evolution of the Martian highlands through ancient fluvial processes, *J. Geophys. Res.*, *98*, 3453–3468, 1993.

Crown, D. A., and R. Greeley, Volcanic geology of Hardriaca Patera and the eastern Hellas region of Mars, *J. Geophys. Res.*, *98*, 3431–3451, 1993.

Crown, D. A., K. H. Price, and R. Greeley, Geologic evolution of the east rim of the Hellas basin, Mars, *Icarus*, *100*, 1–25, 1992.

DeHon, R. A., Geologic map of the Pompeii quadrangle (MTM 20057), Maja Valles region of Mars, *U.S. Geol. Surv. Misc. Invest. Ser., Map I-2203*, scale 1:500,000, 1992.

Dohm, J. M., and K. L. Tanaka, Geology of the Thaumasia region, Mars: Plateau development, valley origins, and magmatic evolution, *Planet. Space Sci.*, *47*, 411–431, 1999.

Dohm, J. M., R. C. Anderson, and K. L. Tanaka, Digital structural mapping of Mars, *Astron. Geophys.*, *39*, 3.20–3.22, 1998.

Dohm, J. M., R. C. Anderson, V. R. Baker, R. G. Strom, G. Komatsu, and T. M. Hare, Pulses of magmatic activity through time: Potential triggers for climatic variations on Mars, *Lunar Planet. Sci.* [CD-ROM], *XXXI*, abstract 1632, 2000a.

Dohm, J. M., R. C. Anderson, V. R. Baker, C. R. Neal, J. C. Ferris, T. M. Hare, K. L. Tanaka, D. H. Scott, J. A. Skinner, and J. E. Klemaszewski, Evolution of the principal magmatic complex of Mars, Tharsis (abstract), paper presented at Tharsis Workshop, Planet. Geol. and Geophys. Program, NASA, Keystone, Colo., Oct. 16–18, 2000b.

Dohm, J. M., R. C. Anderson, V. R. Baker, J. C. Ferris, T. M. Hare, R. G. Strom, L. P. Rudd, J. W. Rice Jr., and D. H. Scott, System of gigantic valleys northwest of Tharsis Montes, Mars: Latent catastrophic flooding, northwest watershed, and implications for northern plains ocean, *Geophys. Res. Lett.*, *27*(21), 3559–3562, 2000c.

Dohm, J. M., V. R. Baker, R. C. Anderson, J. C. Ferris, T. M. Hare, K. L. Tanaka, J. E. Klemaszewski, D. H. Scott, and J. A. Skinner, Martian magmatic-driven hydrothermal sites: Potential sources of energy, water, and life, in *The Concepts and Approaches for Mars Exploration, LPI Contrib. 1062*, pp. 93–94, Lunar and Planet. Inst., Houston, Tex., 2000d.

Dohm, J. M., et al., The Tharsis basin of Mars: A potential source for the outflow channel systems, layered wall deposits of Valles Marineris, and putative oceans or paleolakes (abstract), paper presented at Tharsis Workshop, Planet. Geol. and Geophys. Program, NASA, Keystone, Colo., Oct. 16–18, 2000e.

Dohm, J. M., K. L. Tanaka, and T. M. Hare, Geologic, paleotectonic, and paleoerosional maps of the Thaumasia region, Mars, *U.S. Geol. Surv. Misc. Invest. Ser., Map I-2650*, scale 1:500,000, 2001a.

Dohm, J. M., et al., Latent activity for western Tharsis, Mars: Significant flood record exposed, *J. Geophys. Res.*, *106*, 12,301–12,314, 2001b.

Frey, H., Thaumasia: A fossilized early forming Tharsis uplift, *J. Geophys. Res.*, *84*, 1009–1023, 1979.

Frey, H., and T. D. Grant, Resurfacing history of Tempe Terra and surroundings, *J. Geophys. Res.*, *95*, 14,249–14,263, 1990.

Golombek, M. P., Tharsis tectonics (abstract), paper presented at Tharsis Workshop, Planet. Geol. and Geophys. Program, NASA, Keystone, Colo., Oct. 16–18, 2000.

Golombek, M. P., W. B. Banerdt, and R. J. Phillips, Tectonics of Mars, *Geol. Soc. Am. Abstr. Programs*, *51301*, 2000.

Greeley, R., and J. E. Guest, Geologic map of the eastern equatorial region of Mars, *U.S. Geol. Surv. Misc. Invest. Ser., Map I-1802B*, scale 1:15,000,000, 1987.

Gregg, T. K. P., D. A. Crown, and R. Greeley, Geologic map of part of the Tyrrhana Patera region of Mars (MTM Quadrangle-20252), *U.S. Geol. Surv. Misc. Invest. Ser., Map I-2556*, scale 1:500,000, 1998.

Gulick, V. C., Magmatic intrusions and hydrothermal systems: Implications for the formation of small Martian valleys, Ph.D. thesis, Univ. of Ariz., Tucson, 1993.

Head, J. W., III, H. Hiesinger, M. A. Ivanov, M. A. Kreslavsky, S. Pratt, and B. J. Thompson, Possible ancient oceans on Mars: Evidence from Mars Orbiter Laser Altimeter data, *Science*, *286*, 2134–2137, 1999.

Head, J. W., III, B. M. Webb, B. E. Kortz, and S. Pratt, Syria Planum, Mars: A major volcanic construct in the early history of Tharsis (abstract), paper presented at Tharsis Workshop, Planet. Geol. and Geophys. Program, NASA, Keystone, Colo., Oct. 16–18, 2000.

Jöns, H. P., Arcuate ground undulations, gelifluxion-like features and "front tori" in the northern lowlands on Mars, what do they indicate? (abstract), *Lunar Planet. Sci., XVII*, 404–405, 1986.

Lucchitta, B. K., A. S. McEwen, G. D. Clow, P. E. Geissler, R. B. Singer, R. A. Schultz, and S. W. Squyres, The canyon system on Mars, in *Mars*, edited by H. H. Keiffer et al., pp. 453–492, Univ. of Ariz. Press, Tucson, 1992.

MacKinnon, D. J., and K. L. Tanaka, The impacted Martian crust: Structure, hydrology, and some geologic implications, *J. Geophys. Res.*, *94*, 17,359–17,370, 1989.

Masursky, H., J. M. Boyce, A. J. Dial, G. G. Schaber, and M. E. Strobell, Formation of Martian channels, *J. Geophys. Res.*, *82*, 4016–4038, 1977.

McEwen, A. S., M. C. Malin, M. H. Carr, and W. K. Hartmann, Voluminous volcanism on early Mars revealed in Valles Marineris, *Nature*, *397*, 584–586, 1999.

McKenzie, D., and F. Nimmo, The generation of Martian floods by the melting of ground ice above dykes, *Nature*, *397*, 231–233, 1999.

Milton, D. J., Geologic map of the Lunae Palus quadrangle of Mars, *U.S. Geol. Surv. Misc. Invest. Ser., Map I-894*, scale 1:5,000,000, 1974.

Morris, E. C., and K. L. Tanaka, Geologic map of the Olympus Mons region of Mars, *U.S. Geol. Surv. Misc. Invest. Ser., Map I-2327*, 1994.

Morris, E. C., H. Marsursky, D. S. Applebee, and M. E. Strobell, Geologic maps of science study area 3, Olympus Rupes, Mars (Special MTM 15132 Quadrangle), *U.S. Geol. Surv. Misc. Invest. Ser., Map I-2001*, scale 1:500,000, 1991.

Mouginis-Mark, P. J., Volcano/ground ice interactions in Elysium Planitia, Mars, *Icarus*, *64*, 265–284, 1985.

Nelson, D. M., and R. Greeley, Geology of Xanthe Terra outflow channels and the Mars Pathfinder landing site, *J. Geophys. Res.*, *104*, 8653–8669, 1999.

Newsom, H. E., Hydrothermal alteration of impact melt sheets with implications for Mars, *Icarus*, *44*, 207–216, 1980.

Noreen, E., K. L. Tanaka, M. Chapman, G. Haxel, and L. Gaddis, Late stage magmatic-hydrothermal activity in eastern Tharsis? (abstract), paper presented at Tharsis Workshop, Planet. Geol. and Geophys. Program, NASA, Keystone, Colo., Oct. 16–18, 2000.

Parker, T. J., D. M. Schneeberger, D. C. Pieri, and R. S. Saunders, Geomorphic evidence for ancient seas on Mars, in *Symposium on Mars: Evolution of Its Climate and Atmosphere, LPI Tech. Rep. 87-01*, pp. 96–98, Lunar and Planet. Inst., Houston, Tex., 1987.

Parker, T. J., D. S. Gorsline, R. S. Saunders, D. C. Pieri, and D. M. Schneeberger, Coastal geomorphology of the Martian northern plains, *J. Geophys. Res.*, *98*, 11,061–11,078, 1993.

Pieri, D. C., Geomorphology of Martian valleys, in *Advances in Planetary Geology, NASA Tech. Memo.*, *81979*, 1–160, 1980.

Plescia, J. B., and R. S. Saunders, Tectonic history of the Tharsis region, Mars, *J. Geophys. Res.*, *87*, 9775–9791, 1982.

Plescia, J. B., L. E. Roth, and R. S. Saunders, Tectonic features of southeast Tharsis, in *Reports of Planetary Geology Program, NASA Tech. Memo.*, *81776*, 68–70, 1980.

Rice, J. R., Jr., and R. A. DeHon, Geologic map of the Darvel Quadrangle (MTM 20052), Maja Valles region of Mars, *U.S. Geol. Surv. Misc. Invest. Ser., Map I-2432*, scale 1:500,000, 1996.

Richardson, W. P., E. A. Okal, and S. Van der Lee, Rayleigh-wave tomography of the Ontong-Java Plateau, *Phys. Earth Planet. Inter.*, *118*, 29–51, 2000.

Robinson, M. S., P. J. Mouginis-Mark, J. R. Zimbelman, S. S. C. Wu, K. K. Ablin, and A. E. Howington-Kraus, Chronology, eruption duration, and atmospheric contribution of the Martian volcano Apollinaris Patera, *Icarus*, *104*, 301–323, 1993.

Rotto, S. L., and K. L. Tanaka, Geologic/geomorphologic map of the Chryse Planitia region of Mars, *U.S. Geol. Surv. Misc. Invest. Ser., Map I-2441*, scale 1:5,000,000, 1995.

Saar, M. O., and M. Manga, Permeability-porosity relationship in vesicular basalts, *Geophys. Res. Lett.*, *26*, 111–114, 1999.

Schubert, G., S. C. Solomon, D. L. Turcotte, M. J. Drake, and N. H. Sleep, Origin and thermal evolution of Mars, in *Mars*, edited by H. H. Keiffer et al., pp. 147–183, Univ. of Ariz. Press, Tucson, 1992.

Schultz, R. A., and K. L. Tanaka, Lithospheric-scale buckling and thrust structures on Mars: The Coprates rise and south Tharsis ridge belt, *J. Geophys. Res.*, *99*, 8371–8385, 1994.

Scott, D. H., Geologic map of the MTM 25057 and 25052 quadrangles, Kasei Valles region of Mars, *U.S. Geol. Surv. Misc. Invest. Ser., I-Map 2208*, scale 1:500,000, 1993.

Scott, D. H., and J. M. Dohm, Faults and ridges: Historical development in Tempe Terra and Ulysses Patera regions of Mars, *Proc. Lunar Planet. Sci. Conf. 20th*, 503–513, 1990a.

Scott, D. H., and J. M. Dohm, Tectonic setting of Martian volcanoes and deep-seated intrusives, in *MEVTV Workshop "Evolution on Magma Bodies on Mars,"* pp. 39–40, Lunar and Planet. Inst., Houston, Tex., 1990b.

Scott, D. H., and J. M. Dohm, Mars: Structural geology and tectonics, in *Encyclopedia of Planetary Sciences*, edited by J. H. Shirley and R. W. Fairbridge, pp. 461–463, Van Nostrand Reinhold, New York, 1997.

Scott, D. H., and K. L. Tanaka, Geologic map of the western equatorial region of Mars, *U.S. Geol. Surv. Misc. Invest. Ser., Map I-1802-A*, scale 1:15,000,000, 1986.

Scott, D. H., and J. R. Zimbelman, Geologic map of Arsia Mons volcano, Mars, *U.S. Geol. Surv. Misc. Invest. Ser., Map I-2480*, scale 1:1,000,000, 1995.

Scott, D. H., J. M. Dohm, and D. J. Applebee, Geologic map of science study area 8, Apollinaris Patera region of Mars, *U.S. Geol. Surv. Misc. Invest. Ser., Map I-2351*, scale 1:500,000, 1993.

Scott, D. H., J. M. Dohm, and J. W. Rice Jr., Map of Mars showing channels and possible paleolake basins, *U.S. Geol. Surv. Misc. Invest. Ser., Map I-2461*, scale 1:30,000,000, 1995.

Scott, D. H., J. M. Dohm, and J. R. Zimbelman, Geologic map of Pavonis Mons volcano, Mars, *U.S. Geol. Surv. Misc. Invest. Ser., Map I-2561*, scale 1:1,000,000, 1998.

Sleep, N. H., Martian plate tectonics, *J. Geophys. Res.*, *99*, 5639–5655, 1994.

Solomon, S. C., and J. W. Head, Evolution of the Tharsis Province of Mars: The importance of heterogeneous lithospheric thickness and volcanic construction, *J. Geophys. Res.*, *87*, 9755–9774, 1982.

Solomon, S. C., and J. W. Head, The nature and evolution of Tharsis: Global context and new insights from MGS observations (abstract), paper presented at Tharsis Workshop, Planet. Geol. and Geophys. Program, NASA, Keystone, Colo., Oct. 16–18, 2000.

Tanaka, K. L., The stratigraphy of Mars, *Proc. Lunar Planet. Sci. Conf. 17th*, Part 1, *J. Geophys. Res.*, *91*, suppl., E139–E158, 1986.

Tanaka, K. L., Tectonic history of the Alba Patera-Ceraunius Fossae region of Mars, *Proc. Lunar Planet. Sci. Conf. 20th*, 515–523, 1990.

Tanaka, K. L., and P. A. Davis, Tectonic history of the Syria Planum province of Mars, *J. Geophys. Res.*, *93*, 14,893–14,917, 1988.

Tanaka, K. L., J. M. Dohm, J. H. Lias, and T. M. Hare, Erosional valleys in the Thaumasia region of Mars: Hydrothermal and seismic origins, *J. Geophys. Res.*, *103*, 31,407–31,419, 1998.

Tanaka, K. L., J. M. Dohm, J. C. Ferris, and R. C. Anderson, Erosional mechanism for the development of Valles Marineris (abstract), paper presented at Tharsis Workshop, Planet. Geol. and Geophys. Program, NASA, Keystone, Colo., Oct. 16–18, 2000.

Tanaka, K. L., W. B. Banerdt, J. S. Kargel, and N. Hoffman, Huge, CO_2-charged debris-flow deposit and tectonic sagging in the northern plains of Mars, *Geology*, *29*, 427–430, 2001.

Wise, D. U., M. P. Golombek, and G. E. McGill, Tharsis province of Mars: Geologic sequence, geometry, and a deformation mechanism, *Icarus*, *38*, 456–472, 1979.

Witbeck, N. E., K. L. Tanaka, and D. H. Scott, Geologic map of the Valles Marineris region, Mars (east half and west half), *U.S. Geol. Surv. Misc. Invest. Ser., Map I-2010*, scale 1:2,000,000, 1991.

Zimbelman, J. R., S. E. H. Sakimoto, and H. Frey, Evidence for a fluvial contribution to the complex story of the Medusae Fossae Formation on Mars, *Geol. Soc. Am. Abstr. Programs*, *50423*, 2000.

R. C. Anderson, Jet Propulsion Laboratory, Pasadena, CA 91109, USA.

V. R. Baker, J. M. Dohm, and J. C. Ferris, Department of Hydrology and Water Resources, University of Arizona, Tucson, AZ 85721, USA. (jmd@hwr.arizona.edu)

N. G. Barlow, Robinson Observatory, Department of Physics, University of Central Florida, Orlando, FL 32816, USA.

T. M. Hare and K. L. Tanaka, U.S. Geological Survey, 2255 North Gemini Drive, Flagstaff, AZ 86001, USA.

J. E. Klemaszewski, Department of Geology, Arizona State University, Tempe, AZ 85287, USA.

R. G. Strom, Lunar and Planetary Laboratory, Department of Planetary Science, University of Arizona, Tucson, AZ 85721, USA.

(Received February 9, 2001; revised August 9, 2001;
accepted August 22, 2001.)